タイトル	Efficacy of fractal analysis for objective and quantitative evaluation of echocardiographic still images: A retrospective study
別タイトル	心臓超音波検査の客観的・定量的評価におけるフラクタル解析の有効性について:レトロスペクティブスタディ
作成者（著者）	竹内, 泰三
公開者	東邦大学
発行日	2023.03.14
掲載情報	東邦大学大学院医学研究科 博士論文.
資料種別	学位論文
内容記述	主査 : 池田隆徳 / タイトル : Efficacy of fractal analysis for objective and quantitative evaluation of echocardiographic still images: A retrospective study /著者 : Taizo Takeuchi, Fumiya Komatsu, Yoshihisa Urita, Jun-ichi Yamazaki /掲載誌 : Toho Journal of Medicine /巻号・発行年等 : 8(4): 119-128, 2022 /本文ファイル: 出版社版
著者版フラグ	ETD
報告番号	32661甲第1055号
学位記番号	甲第727号
学位授与年月日	2023.03.14
学位授与機関	東邦大学
DOI	info:doi/10.14994/tohojmed.2022-011
メタデータのＵＲＬ	https://mylibrary.toho-u.ac.jp/webopac/TD75739373

Original Article

Efficacy of Fractal Analysis for Objective and Quantitative Evaluation of Echocardiographic Still Images: A Retrospective Study

Taizo Takeuchi[1)] Fumiya Komatsu[1)*] Yoshihisa Urita[1)] and Jun-ichi Yamazaki[2)]

[1)]Department of General Medicine and Emergency Care, Toho University Graduate School of Medicine, Tokyo, Japan

[2)]Department of Nutrition, Kiryu University, Gunma, Japan

ABSTRACT

Introduction: Fractal analysis can be used to quantify data from medical images by calculating the fractal dimensions of structures. The method is based on the self-similarity of biological structures. We hypothesized that the fractal dimensions calculated from ultrasonographic images would fluctuate in heart disease. We investigated the application of fractal analysis for quantitative evaluation of ultrasonographic images of the myocardium.

Methods: A total of 1000 individuals who underwent echocardiography between January 2003 and December 2020 were enrolled in this retrospective study. Participants were categorized as "diseased," with reduced left ventricular ejection fraction (LVEF), and normal. Causes of reduced LVEF included ischemic heart disease, cardiomyopathy, valvular heart diseases, arrhythmia, or unknown etiologies. Fractal dimensions were calculated from echocardiographic images acquired in motion mode. The region of interest was set as the ventricular septum or posterior wall in systole or diastole, respectively. Fractal analysis was performed using the box-counting method.

Results: The fractal dimension of the ventricular septum and posterior wall were significantly larger in systole than in diastole among normal participants. The fractal dimension of the ventricular septum was larger in diastolic outline mode among diseased participants. However, the fractal dimension of the ventricular septum and posterior wall was decreased in systolic outline for the diseased group.

Conclusions: Fractal analysis of echocardiographic images may be useful for performing quantitative evaluations of myocardium impairment. This noninvasive method using still images is easily applicable in clinical settings.

Toho J Med 8 (4): 119–128, 2022

KEYWORDS: echocardiography, fractal dimension, left ventricular ejection fraction, still image

*Corresponding Author: Fumiya Komatsu, 6-11-1 Omorinishi, Ota-ku, Tokyo 143-8541, Japan, tel: 03–3762–4151
e-mail: fumiya.komatsu@med.toho-u.ac.jp
DOI: 10.14994/tohojmed.2022-011

Received Mar. 31, 2022: Accepted June 6, 2022
Toho Journal of Medicine 8 (4), Dec. 1, 2022.
ISSN 2189–1990, CODEN: TJMOA2

Table 1-a Characteristics of the normal and diseased groups

	Normal hearts	Diseased hearts	p
No.	500	500	
Mean age (y)	70.0 ± 16	71.0 ± 15	0.66
M/F ratio	67.20%	44.40%	< 0.001 *
Male	222	336	
Female	278	164	< 0.001 *
EF (%)	72.1 ± 4	43.4 ± 10	< 0.001 *

* $p < 0.05$
EF = left ventricular ejection fraction

Introduction

Echocardiography can be used to evaluate morphological changes and cardiac function simultaneously by analyzing moving images. In general, morphological changes are evaluated by measuring the aortic and left-atrial diameters on still images. The left ventricular ejection fraction (LVEF) is expressed as the ratio of the left ventricular stroke volume to the left ventricular end-diastolic volume. An echocardiogram is a real-time picture of the heart and so provides useful insight into heart function. However, the site of myocardial damage is not always the same as the hypokinetic site observed by echocardiography. Moreover, it is difficult to assess the impaired site of the myocardial wall without additional cardiac catheterization or nuclear medicine examination. Changes in the structure and function of the heart muscle in combination with certain conditions such as diabetes mellitus, chronic kidney diseases, or hypertension can result to irreversible heart disease. Early detection may enable the prevention of progression, but obtaining sufficient medical information, such as real-time moving images, is not always possible, and clinicians must work with the limited medical information available in clinical settings. Morphological diagnoses can be made from still medical images from modalities such as ultrasonography, computed tomography (CT), magnetic resonance imaging (MRI), and endoscopy. Except for echocardiogram, many of these modalities may be used to evaluate morphological changes associated with tissue damages. Still images can also be analyzed to estimate the effects of diffuse diseases such as hepatitis and thyroiditis and can be used to reveal tissue damage in cardiac muscle cells. Currently, analysis of cardiac muscle damage using still images from echocardiography is limited.

Fractal analysis is one method that is used to evaluate the tightness of a whole structure using self-similarity in which tightness is quantified in terms of fractal dimensions. In our department, we have used mathematical analysis on models of the spread of methicillin-resistant *Staphylococcus aureus* infection, the development of reflux esophagitis,[1] the treatment of retinal detachment, and the bifurcation of hepatic arterial vessels.[2] Fractal analysis has been used to evaluate bronchial and vascular trajectories,[3] cerebral sulci,[4] gastric fluoroscopic images,[5] chest CT images, brain MRI, and fluorodeoxyglucose-positron emission tomography (FDG-PET) images[6] in living organisms. This involves extracting the contours of cells using images of cell samples and calculating the fractal dimensions of the contours.[7] We also currently perform fractal analysis of ultrasound images to assess thyroid disease.[8] With the insight gained from our previous work, we now propose a new method for the objective analysis static images obtained by echocardiography to clarify the impaired site within the cardiac muscle.

Methods

Data acquisition

We collected ultrasound images of all patients who underwent echocardiography using motion (M)-mode between January 2003 and December 2020 whose data were deposited in the database of Toho University Omori Medical Center. Patients were categorized as normal or diseased (Table 1). Disease was defined by an ejection fraction (EF) of < 55%, which was calculated using the Teichholz formula.[9] The disease group was then divided into five subgroups, namely, ischemic heart disease, cardiomyopathy, valvular disease, arrhythmia, and unknown cause.

Principle of fractal analysis

Mandelbrot[10–12] identified self-similarity in complex structures in nature and proposed that these structures could be formulated as fractal dimensions. One example of a fractal is the Koch curve.[13,14] To formulate a structure as fractal dimensions, a straight line is first divided into three equal segments. The middle segment is then replaced with two sides of an equilateral triangle of the same length as the segment being removed. The four resulting segments are divided into three equal parts and each of the middle segments replaced with two sides of an equilateral triangle. The segment is now the same shape as the whole

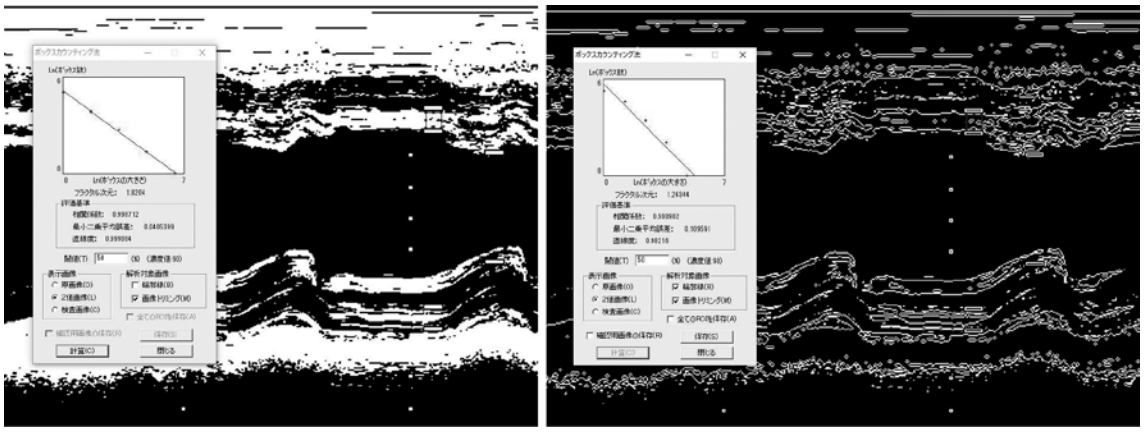

Fig. 1 Images depicting the implementation method of fractal analysis using echocardiographic still images (left: mass mode, right: outline mode). The region of interest was drawn using the contours of the ventricular septum and posterior wall as boundaries, extracted using motion (M)-mode. Mass mode is defined as the maximum value obtained by setting the density threshold. Outline mode emphasizes the outline of the object by analyzing the complexity of the real outline.

and this is referred to as self-similarity. When the whole is divided into N parts using the similarity ratio R, D = −log N/log R represents the similarity dimension. Familiar examples of self-similarity are line segments, squares, and cubes. Bisecting a side divides a line segment into two, a square into four, and a cube into eight similar shapes; thus, for a line segment, R = 1/2 and N = 2; so, D = 1. For a square, R = 1/2 and N = 4; so, D = 2. For a cube, R = 1/2 and N = 8; so, D = 3. This is consistent with the empirical dimensions of each figure. In the Koch curve, R = 1/3 and N = 4; so, D = log4/log3 ≈ 1.2618, which is expressed as a non-integer.[13] Nature does not exhibit perfect fractal structures.

Various methods can be used to determine the fractal dimension. In medical image analysis, fractal dimensions are most commonly calculated using the box-counting method.[9, 14] This method has also been reported by Russell et al. .[15, 16] The fractal dimension is calculated from the slope of log(N(c)) with respect to log(c) as a function of c, counting the number of squares N(c) that contain the target point or line when the target image is covered by a square with side c.[9, 14]

Measurement of fractal dimension

We acquired M-mode ultrasound images using a 1-5 MHz sector array transducer; either a Vivid-E95 (GE Healthcare), Vivid-I (GE Healthcare) Vivid-S70N (GE Healthcare), IE-33 (Phillips Healthcare), EPIQ-7C (Phillips Healthcare), or Affniti-70 G (Phillips Healthcare). The region of interest (ROI) was set as the systole and diastole of the ventricular septum and posterior wall and was extracted by M-mode. The region was then selected using a short shape. Determining the ROI is important for fractal analysis. The ventricular septum and posterior wall are set when measuring LVEF using M-mode. In this fractal analysis, the ROI was set as the area where LVEF was measured in M-mode to improve reproducibility. Echocardiographic images were analyzed using fractal analysis software (Custom Fractal version 1.00; DBkids, PopImaging, Kanagawa, Japan). We used the box-counting method to obtain the fractal dimension of the tissue contour depicted in the ultrasound image. First, electronic cardiac ultrasound images were converted to 8-bit grayscale images, which were then converted into black/white images through binarization. Pixels were converted to white if the gray value was equal to or greater than the threshold or to black if smaller. The threshold was determined automatically by the fractal analysis software, based on the content of the image. Images were then sequentially divided into small areas of 1(= 2^0), 2(= 2^1), 4(= 2^2), 8(= 2^3), and r(= 2^n) in terms of the size of one side of the small area, and the number of small areas containing the target figure, N(r), was calculated respectively. The least-squares method was used to find the value of D that satisfies the equation $N(r) = K \times r^{-D}$. This value is the fractal dimension. These operations were performed in mass mode (Fig. 1, left) and outline mode (Fig. 1, right).

Statistical analysis

The fractal dimension for each group is presented as the mean value with 95% confidence limits. All statistical analyses were performed using Easy R (EZR) (Saitama

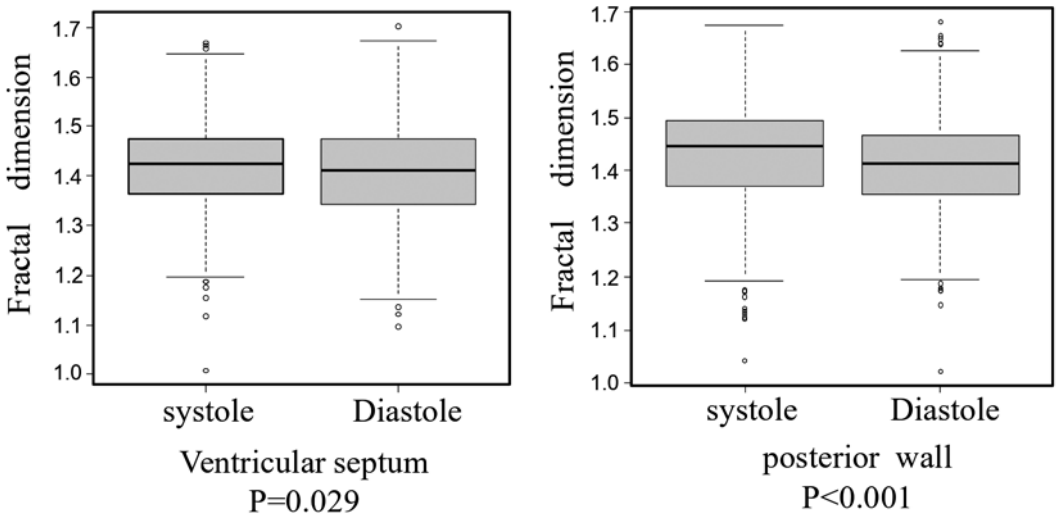

Fig. 2 Box and whisker plots showing the fractal dimensions of the ventricular septum and posterior wall in systole and diastole calculated using data from healthy individuals acquired using outline mode. We used the Mann-Whitney U test.

Medical Center, Jichi Medical University, Saitama, Japan), a graphical user interface for R (The R Foundation for Statistical Computing, Vienna, Austria). We used Mann-Whitney U test to analyze the fractal dimension to compare normal and diseased groups, systolic and diastolic patients within the normal group, and male and female patients. We used the Kruskal-Wallis test and the Steel-Dwass test to analyze fractal dimension according to age. For the proportion of male and female, we used the chi-square test. A p-value of < 0.05 was considered significant.

Results

Comparison of fractal dimension between systole and diastole in normal heart group

We enrolled 1000 participants for this study, 558 males (55.8%) and 442 females, with a mean age of 70.4 years (range 20-100 years) (Table 1). The mean age in the normal and disease groups was 70.0 and 71.0 years, respectively. The male/female ratio in the disease group was 67.2% (336/164) and significantly higher (44.4%, 222/278) in the normal group ($P < 0.001$). The most common disease was unknown cause (18.1%), followed by ischemic heart disease (16.5%), arrhythmic heart disease (5.7%), cardiomyopathy (5.2%), and valvular disease (4.5%).

The fractal dimension was calculated for systole and diastole among normal participants. When the ROI was placed at the ventricular septum and posterior wall and analyzed using outline mode, the fractal dimension was significantly larger in systole than in diastole (Fig. 2). When using outline mode, the mean values of the ventricular septum in systole and diastole were significantly different (1.425, [1.362-1.476] and 1.410 [1.343-1.475], $p = 0.029$). The mean values of the posterior wall were 1.445 [1.369-1.494] and 1.414 [1.356-1.467] in systole and diastole, respectively, which were also significantly different ($p < 0.001$).

The fractal dimension of posterior wall was significantly larger in diastole than in systole when analyzed in mass mode (1.804 [1.796-1.812] versus 1.796 [1.780-1.812], respectively; $p < 0.001$). There was no significant difference in fractal dimension between systole and diastole when the ROI was placed at the ventricular septum.

Fractal dimension of normal and diseased groups

Table 2 shows the comparison of calculated fractal dimension between the diseased and normal groups. When the ROI was placed at the ventricular septum, there was no significant difference in diastolic mass mode (1.799 [1.793-1.811] and 1.796 [1.786-1.811], respectively; $P = 0.395$) (Fig. 3-a). When using outline mode, the values were 1.410 [1.342-1.474] and 1.422 [1.357-1.480] for the normal and diseased groups in diastole, respectively ($p = 0.029$) (Fig. 3-b). During systole, the median values obtained using mass mode were 1.796 [1.794-1.811] and 1.804 [1.788-1.811] for the normal and diseased groups, respectively ($p = 0.687$) (Fig. 3-c). The values obtained using outline mode were 1.425 [1.361-1.475] and 1.407 [1.343-1.460], for the normal and diseased groups, respectively ($p < 0.01$) (Fig. 3-d). When analyzing the posterior wall, a significant difference in fractal dimension was found in only the values obtained using out-

Table 2 Fractal dimensions calculated using mass and outline mode for the normal and diseased groups

		Mass mode [95% CI]					Outline mode [95% CI]				
		Diastole	p	Systole	p		Diastole	p	Systole	p	
Ventricular Sep	Normal	1.799 [1.793–1.811]	0.395	1.796 [1.794–1.811]	0.687		1.41 [1.342–1.474]	0.029 *	1.425 [1.361–1.475]	0.003 *	
	Disease	1.796 [1.786–1.811]		1.804 [1.788–1.811]			1.422 [1.357–1.480]		1.407 [1.343–1.460]		
Posterior wall	Normal	1.804 [1.796–1.811]	0.158	1.796 [1.780–1.811]	0.126		1.414 [1.356–1.467]	0.629	1.444 [1.369–1.494]	0.005 *	
	Disease	1.796 [1.787–1.811]		1.796 [1.785–1.811]			1.418 [1.356–1.471]		1.416 [1.356–1.474]		

We used the Mann-Whitney U test.
* $p<0.05$
Ventricular Sep = ventricular septum

line mode during systole. The values were 1.444 [1.369-1.494] and 1.416 [1.356-1.474], for the normal and diseased groups, respectively ($p < 0.01$).

Comparison of fractal dimension according to age

Age-related changes in cardiac function have been reported.[17] Therefore, we examined age-related changes. The fractal dimension of the ventricular septum during diastole (Fig. 4-a, b) and systole (Fig. 4-c, d) was not significantly different for either the ventricular septum or the posterior wall between any of the age groups (data not shown for the posterior wall). There was no significant difference in fractal dimension by age (diastolic mass mode, $p = 0.239$; diastolic outline mode, $p = 0.654$; systolic mass mode, $p = 0.457$; systolic outline mode, $p = 0.284$).

Comparison of fractal dimension according to gender

Gender differences in cardiac function have also been reported.[18] Therefore, we examined changes in cardiac function by gender. The fractal dimension of the ventricular septum was not significantly different between males and females in the normal group in both diastole (Fig. 5-a, b) and systole (Fig. 5-c, d). When the ROI was placed at the posterior wall, the fractal dimension was significantly larger among males than females in diastolic outline mode (data not shown).

Comparison of fractal dimension according to disease subgroup

The fractal dimension was compared between the normal group and each disease (Table 3). When the ROI was placed at the ventricular septum, the fractal dimension of the ischemic heart disease subgroup significantly increased in diastolic outline mode. When the posterior wall was analyzed, there was no significant difference in fractal dimensions from diastolic outline mode, but in systolic mass mode. There were no significant differences in fractal dimension for the cardiomyopathy, valvular, and arrhythmia subgroups either systole or diastole in any mode.

Discussion

We found that the fractal dimension of the ventricular septum was larger in diastolic outline mode among diseased group when the ROI was placed at the ventricular septum. However, the fractal dimension of the ventricular septum and posterior wall was decreased in systolic outline for the diseased group. This might demonstrate the utility of fractal analysis as a noninvasive and objective method of evaluating regional myocardial damage. Several reports describe the use of fractal analysis in cardiol-

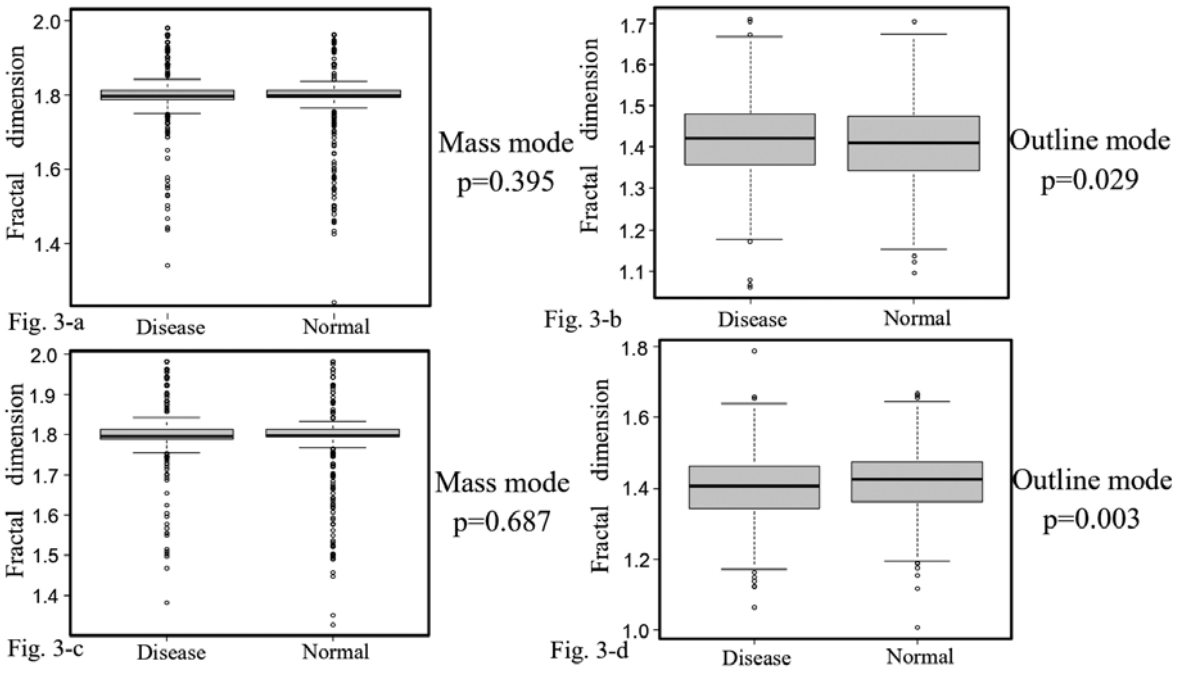

Fig. 3 Box and whisker plots showing the fractal dimensions of the diseased and normal groups calculated in mass and outline modes.
We used the Mann-Whitney U test.

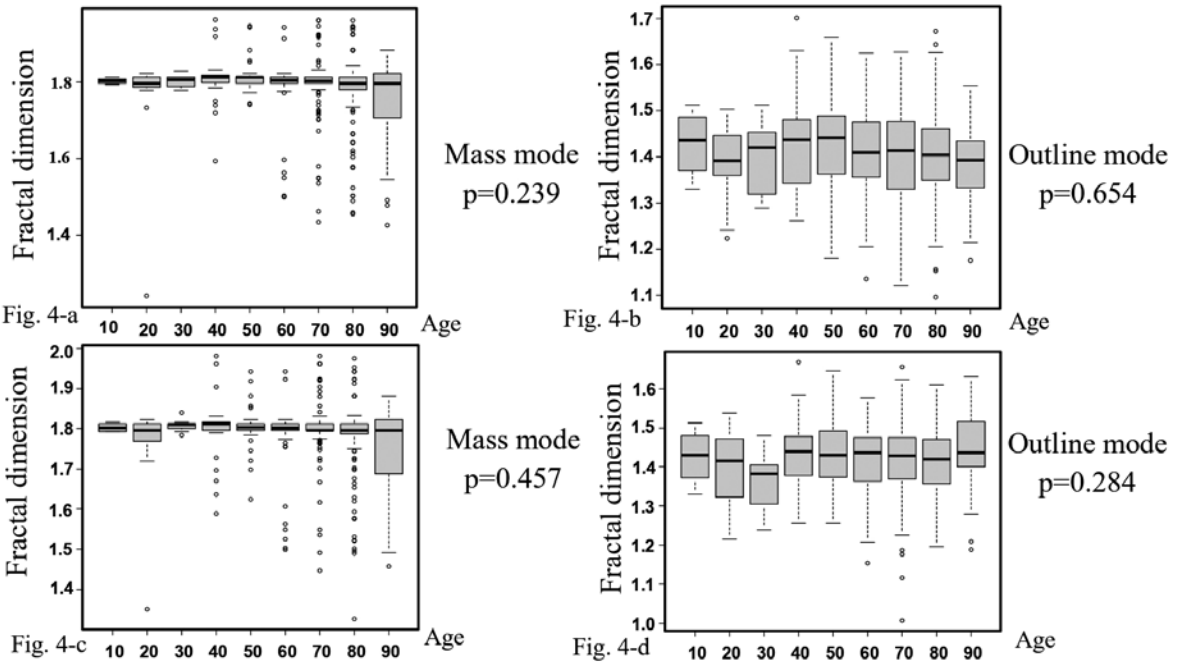

Fig. 4 Box and whisker plots of fractal dimensions calculated in mass and outline modes for each age subgroup within the normal group.
We used the Kruskal-Wallis test and the Steel-Dwass test.

ogy.[8, 19, 20] Cai et al.[19] used fractal analysis to detect myocardial damage on cardiac MRI (CMR) scans from 180 patients with left ventricular non-compaction (LVNC). The authors carried out fractal analysis using a semi-automated technique, which enabled robust measurement of the degree and complexity of left ventricular trabecula-

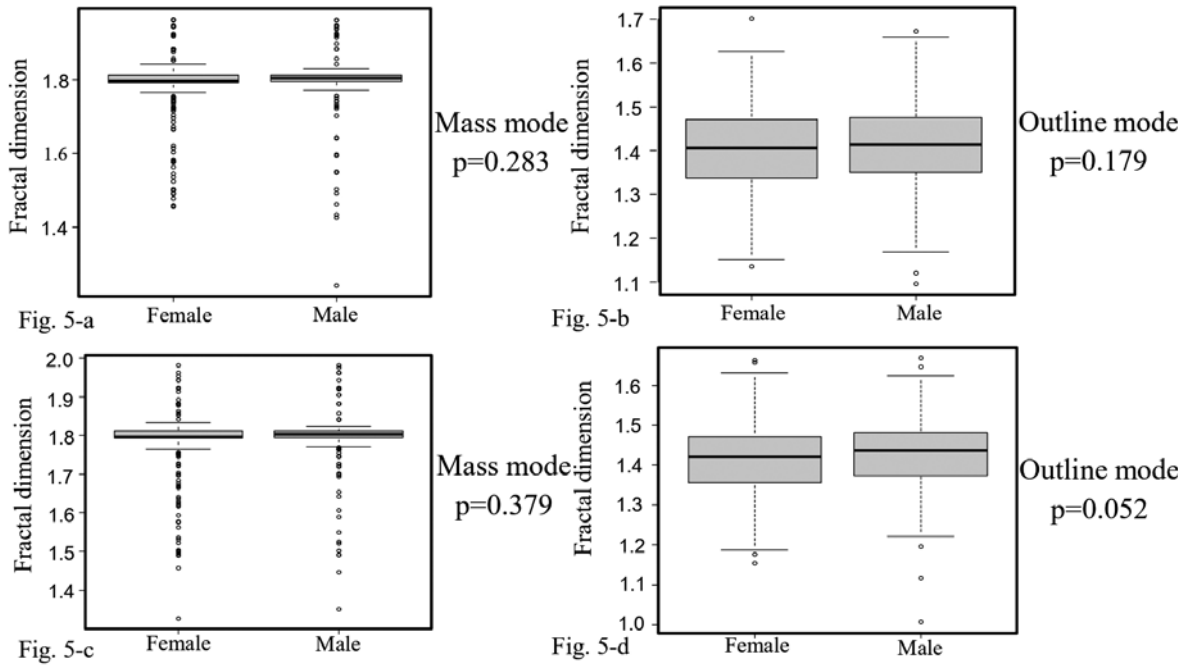

Fig. 5 Box and whisker plots showing the fractal dimensions of ventricular septum calculated in mass and outline modes for each gender.
We used the Mann-Whitney U test.

tion. Fractal analysis is also a reproducible method of assessing the extent of densification disorders ICC through global fractal dimension. In this study, all patients with abnormally high fractal dimension had a definitive diagnosis of LVNC. These studies suggest that fractal analysis is a reproducible method of assessment and highlight the association between fractal dimension and myocardial damage. McLachlan et al.[20] carried out fractal analysis of pathological images of rabbits with myocardial infarction to visually determine the border of myocardial infarction. Visualization of the histological changes of the infarct limbus from a rabbit with a transverse medium-sized infarction (occupying 25% of the left ventricular area) revealed differences between the anterior and posterior sides. This was emphasized when the limbus was reconstructed and magnified. The posterior infarct edge was patchy, but the extent of the patchiness was difficult to determine visually and was more densely structured than anterior one. Fractal dimensions of the anterior and posterior margins of the infarct were 1.16 and 1.29, respectively. Thus, pathologically dense structures may have increased fractal dimensions. In their fractal analysis of thyroid ultrasonographic images, Komatsu et al.[8] highlighted the possibility of noninvasive assessment of thyroid disease. The sagittal section of the thyroid gland was calculated from brightness-mode images from 1205 participants with normal thyroid, Graves' disease, Hashimoto's thyroiditis, subacute thyroiditis, adenomatous disease, papillary carcinoma, or a combination. The fractal dimensions of both contour and concentration structures were significantly reduced for normal thyroids compared with any of the disease groups. Among the disease groups, the fractal dimension was highest in the case of papillary carcinoma, indicating the ability of fractal analysis of ultrasound images to identify changes in organizational structure.

This study revealed the fractal dimension of the ventricular septum of the disease group during systole to be reduced in outline mode. In the fractal dimension, the mass mode evaluates tissue density, whereas the outline mode evaluates the complexity. By evaluating not only density but also complexity, the fractal dimension of the tissue can be evaluated more accurately.[21] Cardiomyocytes, together with skeletal muscle cells, are called rhabdomyosarcoma. They have a stripe pattern, which is perpendicular to the direction of contraction. Each of these stripes is a contractile unit, a "sarcomere".[22,23] Myofibrils are sarcomeres that repeat and align in the direction of contraction and then bundle together to form muscle cells. Sarcomeres are precise structures in which actin and myosin fibers are regularly aligned with partial overlap. Actin fibers are helical,

Table 3 Fractal dimensions calculated for each disease subgroup

		Mass mode [95% CI]				Outline mode [95% CI]			
		Diastole	p	Systole	p	Diastole	p	Systole	p
Normal	Ventricular septum	1.799 [1.793–1.811]		1.796 [1.794–1.811]		1.41 [1.342–1.474]		1.425 [1.361–1.475]	
	Posterior wall	1.804 [1.796–1.811]		1.796 [1.780–1.811]		1.414 [1.356–1.467]		1.444 [1.369–1.494]	
Ischemic heart	Ventricular septum	1.802 [1.794–1.811]	0.588	1.804 [1.794–1.818]	0.208	1.445 [1.373–1.498]	<0.001 *	1.404 [1.336–1.474]	0.076
	Posterior wall	1.797 [1.786–1.812]	0.785	1.797 [1.78–1.811]	0.021 *	1.43 [1.366–1.478]	0.112	1.424 [1.350–1.478]	0.159
Cardiomyopathy	Ventricular septum	1.796 [1.775–1.811]	0.141	1.796 [1.784–1.805]	0.138	1.409 [1.361–1.463]	0.693	1.395 [1.340–1.453]	0.063
	Posterior wall	1.796 [1.786–1.811]	0.314	1.797 [1.792–1.811]	0.421	1.392 [1.335–1.441]	0.099	1.414 [1.367–1.459]	0.081
Valvular	Ventricular septum	1.796 [1.789–1.811]	0.792	1.796 [1.784–1.811]	0.375	1.398 [1.356–1.471]	0.916	1.397 [1.349–1.456]	0.085
	Posterior wall	1.796 [1.774–1.811]	0.067	1.796 [1.777–1.811]	0.855	1.426 [1.360–1.476]	0.624	1.408 [1.342–1.487]	0.279
Arrhythmia	Ventricular septum	1.796 [1.784–1.811]	0.265	1.796 [1.781–1.811]	0.24	1.425 [1.375–1.490]	0.22	1.421 [1.386–1.481]	0.513
	Posterior wall	1.796 [1.794–1.811]	0.471	1.796 [1.784–1.808]	0.983	1.414 [1.367–1.473]	0.653	1.414 [1.360–1.487]	0.344

We used the Mann-Whitney U test.
* $p<0.05$

directionally polymerized monomeric actin fibers, but they are oriented in a fixed direction within the sarcomere. The positive end is connected to the Z line, and the negative end is oriented toward the M line, which represents the center line of the sarcomere. The myosin head is a molecular motor, which protrudes toward the actin fiber and moves toward the positive end of actin fibers using adenosine triphosphate hydrolysis. Therefore, actin fibers are pulled toward the center of the sarcomere, resulting in shortening of the sarcomere and concomitant muscle contraction. Sarcomeres are the contractile apparatus in cardiomyocytes and are the smallest units that make up the contractile system. In normal myocardium, sarcomeres contract and assemble during systole, resulting in a denser structure than in diastole,[24, 25] which is reflected by the fractal dimensions of the normal group in the present study. When the myocardium is damaged, the structure of the sarcomere changes irregularly.[26, 27] In addition, microtubules increase in pressure overload and after myocardial infarction, and the density of myocardium increases.[28] Increased microtubule detyrosination interferes with sarcomere contraction, leading to impaired cardiac contractility.[29] Therefore, the increased fractal dimension that we observed in mass mode could reflect increased microtubule density. In contrast, outline mode evaluates the form and complexity. The decreased fractal dimensions that we observed in the disease group could indicate lower morphological complexity during contraction, as sarcomere shortening is disturbed in impaired cardiac muscle.

When the ROI was placed at the ventricular septum, the fractal dimension of the disease group was increased in outline modes during diastole, seemingly correlating with impaired diastolic function. Cardiomyocytes comprise one-third of the cell population, while the remaining two-thirds are non-cardiomyocytes, mostly fibroblasts. Fibroblasts synthesize and secrete collagen and elastic fibers, which make up the interstitium.[30] Diastolic dysfunction is the inability to dilate due to increased fibrosis of the interstitium and increased myocardial stiffness.[31] Post-myocardial infarction has been reported to lead to myocardial remodeling by increased fibrosis and stiffness of the myocardial interstitium; hence, the interstitial component may influence dilation.[32] The increased fractal dimensions that we observed during diastole in the diseased group are may be due to increased density of the interstitium.

We found significant differences in fractal dimension in the ventricular septum more frequently than in the poste-

rior wall, possibly due to differences in the remodeling and structure of the two structures. The ventricular septum shows predominant ventricular wall thickening compared to the posterior wall due to mechanical and pressure loading,[33, 34] which is a compensatory change to maintain systole function and may appear as an early change in the heart. Structural differences have also been noted between the ventricular septum and posterior wall. The ventricular septum also contains fibers from the right ventricle, which might confer different layer structure, cell size, and interstitial components compared with those from the left ventricle.[35, 36]

We examined the fractal dimension in relation to gender and age because these factors were different between the diseased and normal groups. The fractal dimension of the ventricular septum was not significantly different between different age or gender groups within the normal group. This suggests that age and gender do not affect the pathological structural changes of the ventricular septum.

Fractal analysis is not affected by image magnification, which makes it suitable for retrospective studies using medical images.[37] However, this study has some limitations that should be acknowledged. First, not images were acquired using the same cardiac ultrasound equipment, and there may be differences even within the same tissue. Second, the box-counting method discovered by Russell[38] is the most commonly used method for calculating fractal dimension, but it has been shown to have some limitations, such as reduced estimation accuracy.[39–42] Third, the measurement of EF in echocardiography depends on experience of practitioner and is influenced by the patient's body shape. Therefore, there is a possibility of overestimation or underestimation.[43–45] Finally, the disease group was defined by decreased contractility, but the ongoing process of impaired contractility may have influenced results. Further study is warranted to clarify the relationship between fractal dimension and various myocardial diseases.

The fractal dimension calculated from echocardiographic images changes predominantly in the case of disease. Changes in fractal dimension could be associated with pathological changes of the myocardium. Fractal analysis of still images from echocardiograms can be used as a noninvasive and quantitative assessment.

Acknowledgements/Funding source: This study did not receive any specific grant from the funding agency. Excel data for this study is available from the corresponding author upon request.

Authors' contribution: The primary author contributed to the study design development, data collection, data interpretation, and writing of the manuscript.

Dr. Komatsu contributed to the study design development, data interpretation, and writing of the manuscript.

Dr. Urita contributed to the study design development, data interpretation, and writing of the manuscript.

Dr. Yamazaki contributed to data interpretation and writing of the manuscript.

Ethics statement: The study protocol was approved by the Ethics Committee of Toho University Omori Medical Center (No. M21111 18088 17017). Details about this study were disclosed in our institutional website, and the potential participants were given the opportunity to decline to be further enrolled in the study (opt-out).

Conflicts of interest: None declared.

References

1) Tanaka H, Urita Y, Kawagoe N, Sasaki Y, Watanabe T, Kawaguchi T. A mathematical model of the pathophysiology of reflux esophagitis. Toho J Med. 2016; 2: 8-15.
2) Urita Y, Matsuzaki H, Hachiya A, Katayama M, Kai S, Suzuki M, et al. Optimal branching of hepatic artery in patients with liver cirrhosis. Nihon Shokakibyo Gakkai Zasshi. 1992; 89: 610-5 [in Japanese].
3) Matsuo T, Ohno K. Fractal analysis of human retinal blood vessels. Med Imag Technol. 1997; 15: 592-6.
4) Takeda T. Fractal analysis in neural system. Med Imag Technol. 1997; 15: 603-8.
5) Mekada Y, Hasegawa H, Kasuga M, Nawano S, Miyagawa K. Applications of fractal dimension on double contrast X-ray images of stomach. Med Imag Technol. 1997; 15: 609-14.
6) Chen CC, Daponte JS, Fox MD. Fractal feature analysis and classification in medical imaging. IEEE Trans Med Imaging. 1989; 8: 133-42.
7) Takayasu H, Sato T, Yokoyama T. Application of fractal image analysis to cytologic diagnosis. Med Imag Technol. 1997; 15: 587-91.
8) Komatsu F, Kijima S, Kawagoe N, Maruyama K, Tsuboi K, Urita Y. Quantitative mathematical analysis of thyroid ultrasonography using fractal dimension. Toho J Med. 2020; 6: 20-9.
9) Lang RM, Badano LP, Mor-Avi V, Afilalo J, Armstrong A, Ernande L, et al. Recommendations for cardiac chamber quantification by echocardiography in adults: an update from the American Society of Echocardiography and the European Association of Cardiovascular Imaging. J Am Soc Echocardiogr. 2015; 28: 1-39.e14.
10) Mandelbrot BB, Wallis JR. Computer experiments with fractional Gaussian noises: part 3, mathematical appendix. Water Resour Res. 1969; 5: 260-7.
11) Mandelbrot BB, Wallis JR. Computer experiments with fractional Gaussian noises: part 2, rescaled ranges and spectra. Water Resour Rese. 1969; 5: 242-59.

12) Mandelbrot BB, Wallis JR. Computer experiments with fractional Gaussian noises: part 1, averages and variances. Water Resour Res. 1969; 5: 228-41.
13) Sone M, Takagi M. Fractal and its application to image analysis. J Jpn Soc Photogramm Remote Sens. 1991; 30: 24-9.
14) Toyama H, Uemura K. Fractal dimension analysis in medical images. BME. 1999; 13: 30-8.
15) Liebovitch LS, Toth T. A fast algorithm to determine fractal dimensions by box counting. Phys Lett A. 1989; 141: 386-90.
16) Russell DA, Hanson JD, Ott E. Dimension of strange attractors. Phys Rev Lett. 1980; 45: 1175-8.
17) Daimon M, Watanabe H, Abe Y, Hirata K, Hozumi T, Ishii K, et al. Normal values of echocardiographic parameters in relation to age in a healthy Japanese population: the JAMP study. Circ J. 2008; 72: 1859-66.
18) Salton CJ, Chuang ML, O'Donnell CJ, Kupka MJ, Larson MG, Kissinger KV, et al. Gender differences and normal left ventricular anatomy in an adult population free of hypertension: a cardiovascular magnetic resonance study of the Framingham Heart Study Offspring cohort. J Am Coll Cardiol. 2002; 39: 1055-60.
19) Cai J, Bryant JA, Le TT, Su B, de Marvao AD, O'Regan DP, et al. Fractal analysis of left ventricular trabeculations is associated with impaired myocardial deformation in healthy Chinese. J Cardiovasc Magn Reson. 2017; 19: 102.
20) McLachlan CS, Jelinek HF, Kummerfeld SK, Rummery N, McLachlan PD, Jusuf P, et al. A method to determine the fractal dimension of the cross-sectional jaggedness of the infarct scar edge. Redox Rep. 2000; 5: 119-21.
21) Kiso K, Nishimura Y, Nagao M, Murase K, Takahashi Y, Koizumi M. Example of using Custum Fractal medical image fractal analysis software. Jpn J Nucl Med Technol. 2014; 34: 195-209.
22) Martin TG, Kirk JA. Under construction: the dynamic assembly, maintenance, and degradation of the cardiac sarcomere. J Mol Cell Cardiol. 2020; 148: 89-102.
23) Numata G, Takimoto E, Komuro I. Physiological and molecular mechanism of heart failure pathophysiology: systolic and diastolic function. Heart View. 2018; 22: 307-20.
24) Fukuda N, Sasaki D, Ishiwata S, Kurihara S. Length dependence of tension generation in rat skinned cardiac muscle: role of titin in the Frank-Starling mechanism of the heart. Circulation. 2001; 104: 1639-45.
25) Fukuda N, Wu Y, Farman G, Irving TC, Granzier H. Titin isoform variance and length dependence of activation in skinned bovine cardiac muscle. J Physiol. 2003; 553: 147-54.
26) Yu JG, Russell B. Cardiomyocyte remodeling and sarcomere addition after uniaxial static strain in vitro. J Histochem Cytochem. 2005; 53: 839-44.
27) Müller D, Klamt T, Gentemann L, Heisterkamp A, Kalies SMK. Evaluation of laser induced sarcomere micro-damage: role of damage extent and location in cardiomyocytes. PLoS One. 2021; 16: e0252346.
28) Sato H, Nagai T, Kuppuswamy D, Narishige T, Koide M, Menick DR, et al. Microtubule stabilization in pressure overload cardiac hypertrophy. J Cell Biol. 1997; 139: 963-73.
29) Robison P, Caporizzo MA, Ahmadzadeh H, Bogush AI, Chen CY, Margulies KB, et al. Detyrosinated microtubules buckle and bear load in contracting cardiomyocytes. Science. 2016; 352: aaf0659.
30) Kobayashi M, Shibata N, Yamamoto T, Kawaguchi M. Pathological aspect of end-stage heart failure. Cardiovascular Med-Surg. 2002; 4: 419-25.
31) Burkhoff D, Maurer MS, Packer M. Heart failure with a normal ejection fraction. Is it really a disorder of diastolic function? Circulation. 2003; 107: 656-8.
32) Kurose H. Cardiac fibrosis and fibroblasts. Cells. 2021; 10: 1716.
33) Hess OM, Schneider J, Turina M, Carroll JD, Rothlin M, Krayenbuehl HP. Asymmetric septal hypertrophy in patients with aortic stenosis: an adaptive mechanism or a coexistence of hypertrophic cardiomyopathy? J Am Coll Cardiol. 1983; 1: 783-9.
34) Verdecchia P, Porcellati C, Zampi I, Schillaci G, Gatteschi C, Battistelli M, et al. Asymmetric left ventricular remodeling due to isolated septal thickening in patients with systemic hypertension and normal left ventricular masses. Am. J. Cardiol. 1994; 73: 247-52.
35) Hristov N, Liakopoulos OJ, Buckberg GD, Trummer G. Septal structure and function relationships parallel the left ventricular free wall ascending and descending segments of the helical heart. Eur J Cardiothorac Surg. 2006; 29: 115-25.
36) Sanz J, Sánchez-Quintana D, Bossone E, Bogaard HJ, Naeije R. Anatomy, function, and dysfunction of the right ventricle: JACC state-of-the-art review. J Am Coll Cardiol. 2019; 73: 1463-82.
37) Metze K, Adam RL, Vido JR, Lorand-Metze IGH. The influence of staining characteristics on nuclear texture features in cytology. Anal Quant Cytol Histol. 2009; 31: 241-6.
38) Delides A, Panayiotides I, Alegakis A, Kyroudi A, Banis C, Pavlaki A, et al. Fractal dimension as a prognostic factor for laryngeal carcinoma. Anticancer Res. 2005; 25: 2141-4.
39) Normant F, Tricot C. Method for evaluating the fractal dimension of curves using convex hulls. Phys Rev A. 1991; 43: 6518-25.
40) Appleby S. Multifractal characterization of the distribution pattern of the human population. Geogr Anall. 1996; 28: 147-60.
41) Pruess SA. Some remarks on the numerical estimation of fractal dimension. In: Barton CC, La Pointe PR, editors. Fractals in the Earth Sciences. 1st ed. Boston: Springer US; 1995. p. 65-75.
42) Sato Y. Accurate estimation of fractal dimension of binary images by box-counting method with automatic scale selection. Trans Soc Instrum Control Eng. 2003; 39: 1002-9.
43) Benyounes N, Lang S, Soulat-Dufour L, Obadia M, Gout O, Chevalier G, et al. Can global longitudinal strain predict reduced left ventricular ejection fraction in daily echocardiographic practice? Arch Cardiovasc Dis. 2015; 108: 50-6.
44) Macron L, Lairez O, Nahum J, Berry M, Deal L, Deux JF, et al. Impact of acoustic window on accuracy of longitudinal global strain: a comparison study to cardiac magnetic resonance. Eur J Echocardiogr. 2011; 12: 394-9.
45) Medvedofsky D, Kebed K, Laffin L, Stone J, Addetia K, Lang RM, et al. Reproducibility and experience dependence of echocardiographic indices of left ventricular function: side-by-side comparison of global longitudinal strain and ejection fraction. Echocardiography. 2017; 34: 365-70.